Pd, Cu and Bimetallic PdCu NPs Supported on CNTs and Phosphine-Functionalized Silica: One-Pot Preparation, Characterization and Testing in the Semi-Hydrogenation of Alkynes

Daniel Sánchez-Resa, Jorge Delgado, Maria Dolores Fernández-Martínez, Chloé Didelot, Aimery de Mallmann, Kaï Szeto, Mostafa Taoufik, Carmen Claver, Cyril Godard

Pd, Cu and bimetallic PdCu NPs supported on CNTs and phosphine-functionalized silica: one-pot preparation, characterization and testing in the semi-hydrogenation of alkynes

Daniel Sánchez-Resa,[a] Jorge A. Delgado,[b] Maria Dolores Fernandez-Martinez,[b] Chloé Didelot,[c] Aimery De Mallmann,[c] Kaï C. Szeto,[c] Mostafa Taoufik,*[c] Carmen Claver[a,b] and Cyril Godard,*[a,b].

[a] Departament de Química Física i Inorgánica, Universitat Rovira i Virgili, C/Marceli Domingo 1, 43007 Tarragona, E-mail: cyril.godard@urv.cat

[b] Centre Tecnologic de la Química, C/Marce·lí doming, 43007 Tarragona.

[c] CP2M, COMS team (CNRS-UMR 5128) Université Lyon 1, ESCPE Lyon 43 Boulevard du 11 Novembre 1918, 69626 Villeurbanne Cedex, France

Abstract

Triphenylphosphine stabilized Pd, Cu and PdCu nanocatalysts supported on carbon nanotubes (CNTs) or phosphorus functionalised silica (P-SiO_2) were prepared via a one-pot methodology. The series of P-SiO_2 supported catalysts evidenced sizes of metallic nanoparticles (M-NPs) between 1 and 2.4 nm, smaller than their equivalents on CNTs (2.4 – 2.6 nm). Such a difference in particle size as a function of the support and the metallic composition indicated the more pronounced mediation of the CNTs support during the formation of the M-NPs when compared to the P-SiO_2 support. The series of supported catalysts were tested in the semi-hydrogenation of alkynes providing differences in reactivity that might be correlated with the size and composition the M-NPs and the nature of corresponding support. The carbon supported catalysts displayed in general higher activities than those supported on silica and the bimetallic catalyst PdCu/CNTs were the most selective for the case of alkyl substituted alkynes. This catalyst could moreover be recycled several times without loss of activity nor selectivity.

Keywords*:* Alkyne semi-hydrogenation, Carbon nanotubes, Functionalized silica, Nanoparticles, PdCu

1. Introduction

The study of well-defined metal nanoparticles has focused much attention over the last years due to their applications in fields such as biomedicine, optical electronics, catalysis among others.[1] Several approaches have been employed for the immobilisation of metal nanoparticles onto solid supports such as impregnation, co-precipitation or deposition,[2] however, these methodologies often suffer from a poor control of the particle size and distribution.[3]

In this context, surface organometallic chemistry (SOMC) offers an alternative for the preparation of well-defined heterogeneous catalysts through the grafting of organometallic species or complexes onto the surface hydroxyls of classical supports such as alumina or silica,[4] and more recently on PNP incorporated polystyrene matrix.[5] This methodology may also serve to selectively functionalise conventional supports with organic fragments, for example hydroquinone and triphenyl phosphine.[6] For instance, this approach was employed for the synthesis of rhodium and platinum NPs supported on a phosphorus functionalised silica under mild conditions.[6a] The synthesis consisted in a one-pot methodology in which the metallic precursors were reduced under H_2 atmosphere in the presence of triphenylphosphine and the phosphorus functionalised support (P-SiO_2). Under these conditions, well-dispersed small nanoparticles with a homogeneous particle size distribution (1.2 nm for Rh and 1.6 nm for Pt) were obtained.

Nanostructured carbon materials have been also employed in the last decades as carriers of metal nanoparticles, due to their special properties derived from their surface homogeneity of carbon units. This particularity has made of them ideal candidates for the preparation of model catalysts adequate for systematic studies in catalysis.[7] However, the support has not only the role of diluting or dispersing the active phase, its particular characteristics of porosity, surface chemistry, electronic environment, acidity, among others, frequently play an important role in both the synthesis of the catalyst and in the catalytic performance.[8] For the semi-hydrogenation of alkynes, several reports have provided insights about the support dependence in catalysis.[9] For instance, Kiwi-Minsker and co-workers reported the preparation of a composite material based on Pd nanoparticles supported on carbon nanofibers (CNF) grown on sintered metal fibers (Pd/CNF/SMFInconel).[9b] This material was tested as nanocatalyst in the selective hydrogenation of acetylene and compared with Pd supported on activated carbon fibers (Pd/ACF). The TOF was one order of magnitude higher for Pd/CNF/$SMF_{Inconel}$ as compared to Pd/ACF.This effect was attributed to a strong metal-support interaction of Pd°-nanoparticles with the graphitized CNF. According to the authors, the graphitic nature of this support could promote electron transfer between the conductive CNF and the palladium particles, thus inducing electronic perturbations of the metal then affecting the catalyst activity.

One of the strategies extensively used nowadays for enhancing the catalyst performance in the selective hydrogenation of alkynes consist in the dilution of the highly active palladium phase by a second metal with a low affinity for hydrogen (e.g. Ag, Au, Cu, etc).[1c] The impact of such a dilution can be attributed to electronic or geometric effects.[10] In this regard, palladium based bimetallic formulations such as PdAg,[11] and PdAu,[12] PdPt,[12a] PdRhP,[13] PdB,[14] PdCu[7a, 11a, 15] among others have been reported in this reaction. In particular, bimetallic PdCu formulations have experienced special interest by the scientific community during the last years. For instance, McCue et al. reported the modification of a Cu/Al_2O_3 catalyst by various quantities of Pd precursor resulting in the formation of bimetallic catalysts with surfaces dominated by Cu.[15a] More recently, Radivoy and co-workers reported the selective hydrogenation of terminal

alkynes, under mild reaction conditions (H_2 balloon, 110 °C), promoted by a bimetallic nanocatalyst composed of copper and palladium nanoparticles (5:1 weight ratio) supported on mesostructured silica (MCM-48).[15b] The Cu-PdNPS@MCM-48 catalyst, which demonstrated to be highly chemoselective towards the alkyne functionality, was readily prepared from by a chemical reduction methodology using the chloride salts of Cu and Pd and Li-DTBB as the reducing agent.

In our group very recently was reported a straightforward methodology for the preparation of monometallic (copper and palladium) and bimetallic nanocatalysts (NiCu and PdCu) stabilized by a N-heterocyclic carbene ligand.[7a] Both colloidal and supported nanoparticles (NPs) on carbon nanotubes (CNTs) were prepared via a one-pot synthesis with outstanding control on their size, morphology and composition. These catalysts were evaluated in the selective hydrogenation of alkynes and alkynols. Among the tested catalysts, PdCu/CNTs (1:1 molar ratio) revealed an efficient catalytic system providing high selectivity in the hydrogenations of terminal and internal alkynes. Moreover, this catalyst was tested in the semi-hydrogenation of acetylene in industrially relevant acetylene/ethylene-rich model gas feeds and showed excellent stability even after 40 h of reaction.

In addition to palladium based catalysts, very recently, Fedorov and co-workers reported the high potential of a non-noble metal based catalyst consisting in silica supported copper nanoparticles (capped with phosphorus or carbene ligands), in the semihydrogenation of alkynes.[16] The authors evidenced high activity and alkene selectivity for a series of internal alkynes (at 50 bar H_2 and 60 ºC) depending on the ligand used. In spite of these promising results, the preparation of well-defined metallic copper nanoparticles usually involves the use of expensive copper precursors and complicated synthetic methodologies.[16-17] In view of the previous reports, the development of synthetic methodologies for both, copper nanoparticles and bimetallic combinations of this metal with Pd is of high interest for the semi-hydrogenation of alkynes.

In the present study, a step forward in the understanding of the reactivity in the semi-hydrogenation of alkynes with Pd, Cu and bimetallic PdCu NPs supported in different carriers is presented. To achieve this goal, two series of Pd, Cu or PdCu supported nanocatalysts were prepared on carbon nanotubes (CNTs) and phosphorus functionalized silica support (P-SiO_2), and subsequently tested in the semi-hydrogenation of alkynes. This approach permitted the identification of reactivity patterns in which the support may condition for instance the particle size of the deposited metal nanoparticles with concomitant implications in catalysis.

2. Experimental Section

A series of supported mono (Pd, Cu) and bimetallic catalysts (PdCu) were prepared in THF by reduction/decomposition of the corresponding metallic precursor(s): Mesitylcopper (I) $(CuMes)_4$, $Pd(dba)_2$, under hydrogen in the presence of the carrier and substoichiometric amounts of triphenylphosphine ligand.[1b]

The following paragraphs describe the general methodology when either phosphorus functionalized silica or carbon nanotubes were employed as the carriers. For details on each synthesis see the Supporting Information.

2.1. Catalysts supported on phosphorus functionalised silica

Using a 250 ml Fischer-Porter and under nitrogen atmosphere, 150 mg of the phosphorus functionalised silica (P-SiO_2), 0.07 mmol of metallic precursor(s) (5 wt% vs. support) and 7.4 mg of PPh_3 (0.028 mmol) were dispersed in 30 ml of dry THF. The Fischer-Porter bottle was tightly closed, pressurised with 3 bars of H_2 and magnetically stirred at room temperature during 16 h. The bottle was then depressurised in air and the suspension separated by centrifugation. The supernatant was removed and the solid redispersed with *n*-hexane followed by centrifugation. The washing process was repeated 3 times and the resulting material dried under vacuum. A sample of solid was finally suspended in *n*-hexane and deposited on formvar coated copper grids for TEM analysis.

2.2. Catalysts supported on carbon nanotubes

The synthesis of carbon supported materials was analogous to the one described above (using carbon nanotubes instead of phosphorus functionalized silica), with slight differences in the work-up. After the reaction, the Fischer-Porter bottle was depressurised in air, then 30 mL of dry *n*-hexane was added and the mixture stirred for 20 min. The resulted suspension was sampled for TEM analysis. The rest was then filtered through a Nylon 6,6 membrane, washed with *n*-hexane and the resulting material dried in air.

2.3. General procedure for the semi-hydrogenation of alkynes

Catalytic experiments were carried out in a five-position Parr reactor provided with glass liners. In a typical experiment, the glass tube was charged with 5 mL of THF, the substrate and the corresponding amount of a previously prepared suspension of the nanocatalyst. Hydrogen gas was then introduced at the desired pressure, the magnetic stirring initiated (600 rpm) and the reactor heated at the defined temperature. After a given time, the reactor was depressurised and samples of the tubes were diluted in EtOH and analysed by GC-MS. When necessary, after the sampling, the reactor was closed and pressurised again to continue the reaction.

Recycling experiments were conducted using the PdCu/CNTs catalyst. After the first cycle (described above) the catalyst was separated by centrifugation. The supernatant was removed and analysed by GC-MS while the solid washed three times with 10 ml of cold and deoxygenated hexane, brought to dryness under reduced pressure, and later redispersed in THF. The substrate was then added for the next catalytic cycle.

3. Results and discussion

The CNTs or silica supported M-NPs were synthesised based on previously reported methods.[6a] For each metal involved, the nominal loading was 5 wt%.

Synthesis and characterization of Pd NPs supported on CNTs and P-SiO_2

Supported Pd nanoparticles on CNTs or P-SiO_2 were prepared by decomposition of $Pd(dba)_2$, under 3 bar of hydrogen in the presence of triphenylphosphine (PPh_3) and carbon nanotubes (CNTs) or functionalized silica (P-SiO_2). The reaction was performed at room temperature. The solution turned black after 1 h and the catalysts were isolated by complete removal of the

solvent under vacuum. According to the TEM micrographs (Figure 1), spherical nanoparticles of *ca.* 2.5 nm and 0.9 nm were obtained when supported on CNTs and P-SiO_2 respectively.

a. Pd/CNTs **b. Pd/P-SiO_2**

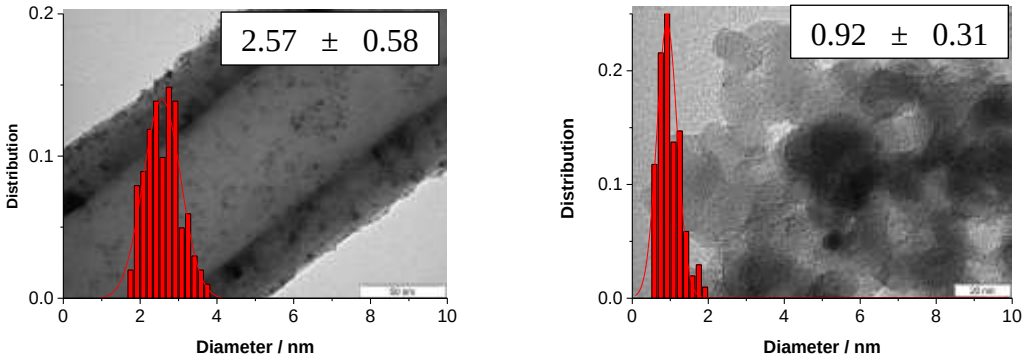

Figure 1. Size histograms and TEM micrographs of **a. Pd/CNTs** and **b. Pd/P-SiO_2**

Considering the ultra-small particle size of the NPs in **Pd/P-SiO_2**, the fine structure of this material was studied by STEM-HAADF. As appreciated in the micrograph (**Erreur ! Source du renvoi introuvable.**), the presence of single atoms and small clusters was detected (indicated in circles) surrounding the small PdNPs. The presence of phosphorus atoms onto the support in combination with the decomposition facility of the Pd precursor might favour the deposition of single atoms or clusters onto the silica surface and the formation of ultra-small NPs. The fine structure of a single nanoparticle of *ca.* 3 nm can be also observed in **Erreur ! Source du renvoi introuvable.**. Analysis of the electron diffraction allowed the identification of two fcc crystallographic planes, 111 and 200, which d-spacings were 2.468 and 2.192 Å, respectively. These values indicate the expansion of the crystalline lattice of the Pd NPs in **Pd/P-SiO_2** catalyst in comparison with the reference values reported for Pd-fcc (see Supporting Information). This behaviour could indicate the doping of the crystalline structure with other atoms, e.g. C or P. For instance, Asakura *et al*. reported the expansion of the crystalline lattice of PVP stabilised Pd-NPs, attributed to the presence of a palladium carbide phase (C doping) formed during the synthesis of the NPs.[18]

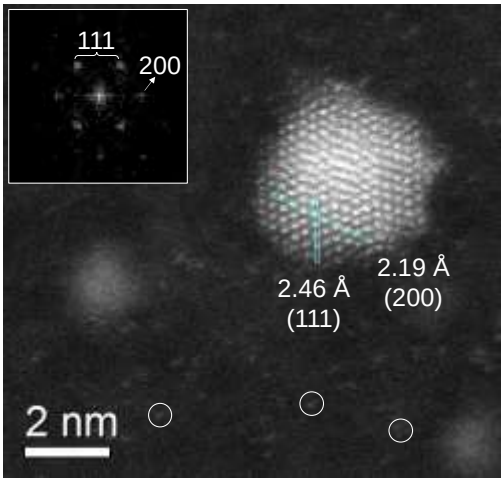

Figure 2. STEM-HAADF micrographs and electron diffraction of a nanoparticle in **Pd/P-SiO_2** catalyst. In circles several Pd single atoms and small clusters are indicated.

The crystalline structure of the synthesised materials was studied by XRD (Supporting information). A defined Pd-fcc structure was observed for **Pd/CNTs**, while the low degree of crystallinity of the **P-SiO$_2$** support in combination with the ultra-small size of the PdNPs did not permitted the detection of metallic diffractions. The metal loading of the prepared materials was determined by ICP. The obtained values for **Pd/CNTs** and **Pd/P-SiO$_2$** were both 4.4 wt%, in close agreement to the nominal value (5 wt%).

Synthesis and characterization of Cu NPs supported on CNTs and P-SiO$_2$

In an analogous manner, supported Cu nanoparticles on CNTs or P-SiO$_2$ were prepared by decomposition of (CuMes)$_4$ under 3 bar of hydrogen in the presence of triphenylphosphine (PPh$_3$) and the support. The reaction was performed at 70ºC. The solution turned black after 3h and the catalysts were isolated by complete removal of the solvent under vacuum. TEM analyses of the obtained materials revealed the formation of spherical NPs of *ca.* 2.4 and 2.1 nm for **Cu/CNTs** and **Cu/P-SiO$_2$** respectively (Figure 3).

a. Cu/CNTs **b. Cu/P-SiO$_2$**

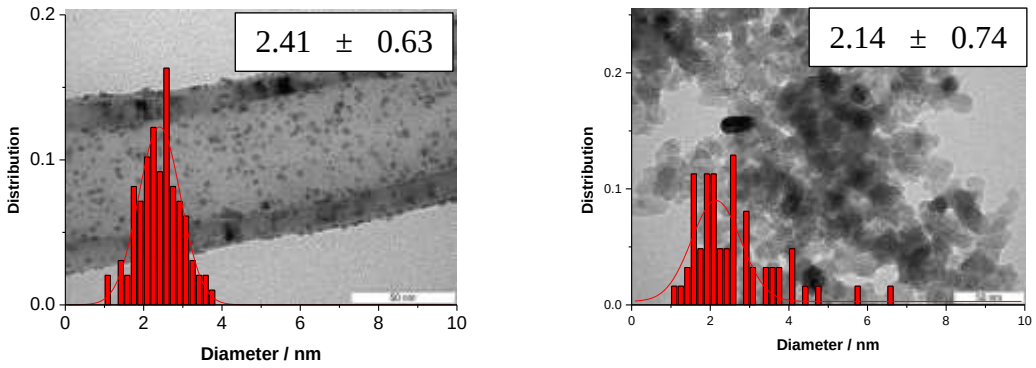

Figure 3. Size histograms and TEM micrographs of **a. Cu/CNTs** and **b. Cu/P-SiO$_2$**

A structural analysis of these catalysts by XRD (Supporting information) evidenced the presence of a peak at 43º assigned to the 111 plane of a Cu-fcc metallic structure. Analysis of the metal loading by ICP indicated values of 6 and 4.8 wt% for **Cu/CNTs** and **Cu/P-SiO$_2$** respectively.

Synthesis and characterization of PdCu NPs supported on CNTs and P-SiO$_2$

Bimetallic PdCu nanoparticles supported on CNTs or P-SiO$_2$ were prepared by decomposition of the corresponding amounts of Pd(dba)$_2$ and (CuMes)$_4$ under 3 bar of hydrogen in the presence of PPh$_3$ and the support (CNTs or P-SiO$_2$). The reaction was performed at 70ºC. TEM analysis of these materials revealed the formation of PdCu NPs of *ca.* 2.6 and 1.5 nm for **PdCu/CNTs** and **PdCu/P-SiO$_2$** respectively (Figure 4).

a. PdCu/CNTs **b. PdCu/P-SiO$_2$**

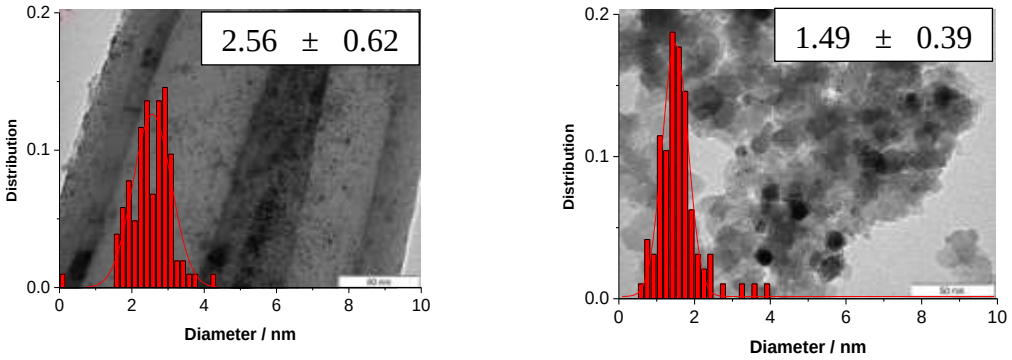

Figure 4. Size histograms and TEM micrographs of **a. PdCu/CNTs** and **b. PdCu/P-SiO$_2$**

The fine structure of the bimetallic catalysts was studied by STEM-HAADF. For the case of **PdCu/CNTs** (Figure 5a), fast Fourier transform (FFT) analysis of single particles permitted the identification and the measure of d-spacing corresponding to the 111 plane (2.251 Å). Microanalyses of several particles by energy dispersive X-ray spectroscopy (EDS) confirmed their bimetallic nature (Supporting Information).

a. **b.**

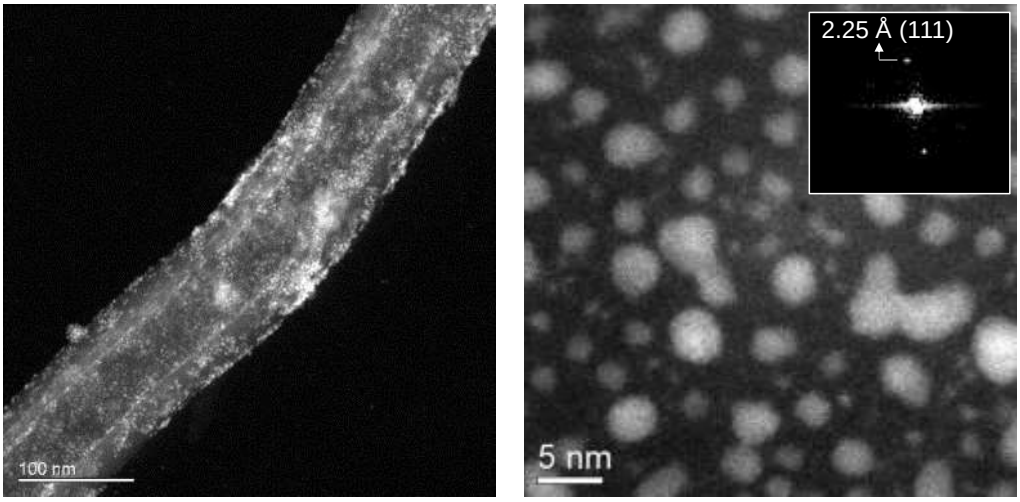

Figure 5. STEM-HAADF micrograph of bimetallic **PdCu/CNTs**. **a.** Low magnification displaying a section of CNT decorated by the NPs. **b.** High magnification; inset corresponds to a representative FFT electron diffraction of a single PdCu NP.

FFT analysis of single particles in **PdCu/P-SiO$_2$** (Figure 6a) permitted the identification and measurement of d-spacing of 2.410 and 2.067 Å, assigned to 111 and 200 planes respectively. These values are slightly smaller when compared to those measured for Pd-NPs in **Pd/P-SiO$_2$** catalyst but significantly larger than reference values for Cu-fcc (2.087 and 1.808 Å for 111 and 200 planes respectively), in agreement with the formation of bimetallic PdCu nanostructures. The metal distribution in a single PdCu NP was studied by EDS of line. According to the observed profile (Figure 6b), the distribution of Pd and Cu was homogeneous along the axes, thus supporting an alloyed structure for these PdCu NPs.

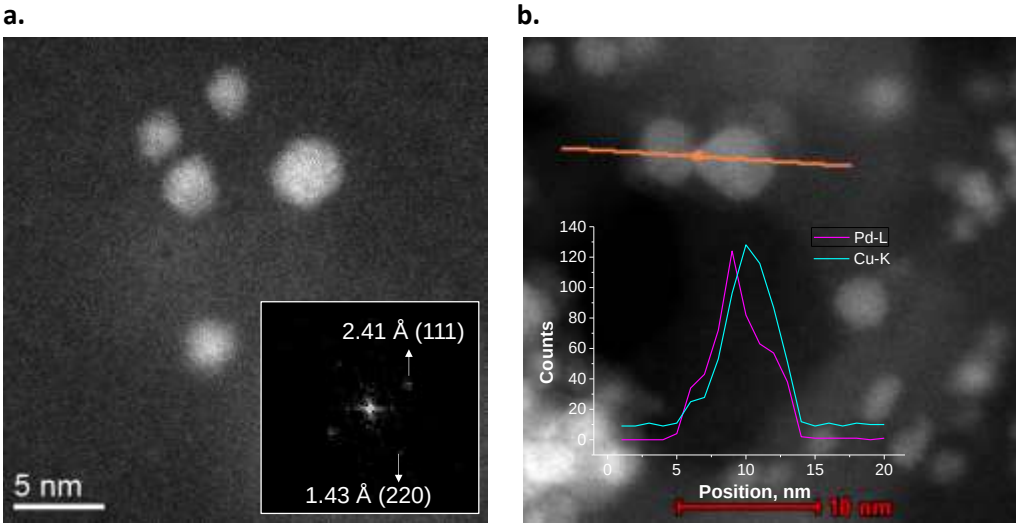

Figure 6. **a.** STEM-HAADF micrograph and electron diffraction (FFT) of several nanoparticles in **PdCu/P-SiO$_2$** catalyst. **b.** STEM-HAADF micrograph of **PdCu/P-SiO$_2$** catalyst; in the inset, EDX elemental analysis of line of a single PdCu particle displaying the counts distribution of Pd-L and Cu-K lines along the axes.

The XRD analysis of **PdCu/CNTs** evidenced the presence of a broad band centred at 43º, which results from the overlapping of the graphitic and metallic diffraction peaks. In contrast, for the case of **PdCu/P-SiO$_2$**, the signals corresponding to PdCu nanocrystals are barely distinguished from the support background due to the amorphous structure of the support in combination with the small size of the NPs. Finally, the metallic loadings measured by ICP for these two catalysts exhibited slightly negative deviations compared to the nominal value (Supporting information).

Summarizing, two main observations can be extracted from the analysis of the particles size for the series of CNTs and P-SiO$_2$ supported catalysts. In first place, comparing catalysts with equivalent metal compositions (e.g **Pd/CNTs** vs. **Pd/P-SiO$_2$**), the NPs supported on the P-SiO$_2$ were always smaller than their homologues on CNTs. The presence of phosphorus atoms on silica might provide additional sites for nucleation of metal clusters during the synthesis, thus favouring the metal dispersion onto the support and therefore the formation of small NPs. This effect is exemplified in **Pd/P-SiO$_2$** where the functionalized support in combination with the decomposition facility of the Pd precursor resulted in the deposition of single atoms, clusters and ultra-small Pd NPs (of less than 1 nm) onto the silica surface. Furthermore, the fact that particle sizes on CNTs supported catalysts converged at *ca.* 2.5 nm might indicate that the CNTs possibly rules the seeding and growth of the deposited NPs independently of the metal composition. For instance, Kiwi-Minsker and co-workers reported the existence of strong metal-support interaction for a Pd catalyst supported on carbon nanofibers (CNFs) and associated it to the graphitic structure inherent to the CNFs.[19] Differently, the particle sizes of the NPs deposited on the series of P-SiO$_2$ supported catalysts followed an order in agreement with the facility of decomposition/reduction of the metal formulations of each case. According to this, the particle sizes were 0.92, 1.49 and 2.14 nm for Pd, PdCu and Cu supported catalysts respectively. Considering that triphenylphosphine was added as a stabilizing agent in all the synthesis, the effect of this ligand on the particle size was discarded. Finally, the bimetallic nature and alloyed structure of the PdCu NPs in the bimetallic catalysts was evidenced.

Catalytic evaluation on the semi-hydrogenation of alkynes

In order to evaluate the reactivity of the different nanocatalysts, four model substrates with defined structural characteristics were tested. The substrates were 1-octyne, 4-octyne, phenylacetylene and diphenylacetylene.

The results of palladium catalysts are displayed in Table 1. For **Pd/CNTs** (entries 1-4), full conversion was observed except for phenylacetylene under the tested conditions. When 1-octyne was the substrate (entry 1), this catalyst displayed a high over-hydrogenation and isomerisation activity after extended reaction times (3 h). For 4-octyne (entry 2), full conversion was achieved after 0.5 h of reaction giving a 88% *cis*-selectivity which decreased to 72% after 3 h of reaction. For this substrate, the catalyst did not undergo over-hydrogenation but exhibited relevant isomerisation (16%). Regarding the aromatic substrates, for phenylacetylene (entry 3) 99% of alkene selectivity at 73% conversion was achieved after 3 h and for diphenylacetylene, full conversion was achieved at 3 h with 100% of alkene selectivity and 92% of *cis*-selectivity.

Pd/P-SiO$_2$ catalyst (entries 5-8), displayed lower activities in comparison to **Pd/CNTs**. When 1-octyne is employed (entry 5), 98% of alkene selectivity at 69% conversion is obtained. For 4-octyne (entry 6) full conversion was achieved with a 97% alkene selectivity and 79% of *cis*-selectivity. For the case of phenylacetylene (entry 7) a low conversion was achieved (30%) meanwhile diphenylacetylene (entry 8) exhibited 100% of alkene selectivity (90% *cis*-selectivity) at 85% conversion.

Table 1. Semi-hydrogenation of alkynes catalysed by Pd based catalysts: **Pd/CNTs** (entries 1-4) and **Pd/P-SiO$_2$** (entries 5-8).[a]

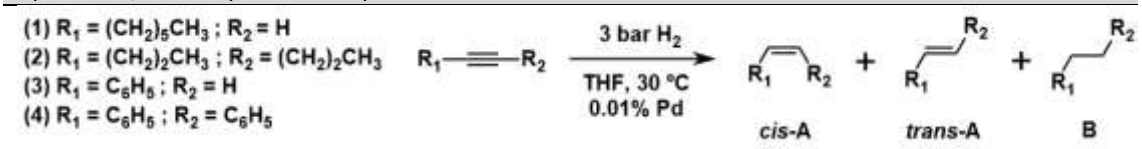

Entry	Substrate	t, h	Conv.%	Sel. Alkene %	Sel. B %	Sel. Isomers %	*Cis*:*Trans*
1	**1**	1.5	100	92	4	4	-
		3	100	5	41	54	-
2	**2**	0.5	100	99	0	1	87:13
		3	100	84	0	16	72:28
3	**3**	3	73	99	1	0	-
4	**4**	3	100	100	0	0	92:8
5	**1**	3	70	98	0	2	-
6	**2**	1.5	100	97	0	3	79:21
7	**3**	3	30	92	8	0	-
8	**4**	3	85	100	0	0	90:10

[a]Reaction conditions: 1.35 mmol of substrate, 0.01 mol% Pd, 5 mL THF, 600 rpm, 3 bar of H_2. Entries 1-4 for **Pd/CNTs** and 5-8 for **Pd/P-SiO$_2$**. Conversions and selectivities were determined by GC-MS spectrometry.

The lower activities observed for **Pd/P-SiO$_2$** catalysts (entries 5-8) were attributed to the differences in size of the Pd NPs, (0.92 and 2.56 nm respectively), considering the well-known structure sensitivity (or particle size effect) operative in the selective hydrogenation of alkynes

and to an effect of the support (SiO_2 vs CNT).[20] Kiwi-Minster *et al*.[20b] studied the structure sensitivity of unsupported Pd NPs with diameters in the range 6-14 nm for the semi-hydrogenation of 1-hexyne. A progressive increase of the activity was observed when the diameter of the nanoparticles increased. The authors attributed this behaviour to the increase in the fraction of low index planes (faces) in larger NPs considering that such sites (Pd100) are more active in the hydrogenation of alkynes. Moreover, the same authors reported an increase in TOF values of one order of magnitude using palladium nanoparticles supported on carbon nanofibers grown on sintered metal fibers (CNF/SMF) rather than Pd catalyst prepared on amorphous active carbon fibers (ACF).[19] This phenomenon was attributed to the stronger metal-support interaction of Pd-CNF/CNF due to the graphitic nature of CNF. According to the authors, electron transfer between the conductive CNF support and the palladium particles might induce electronic perturbations of the metal, thus explaining the activity enhancement. Therefore, the larger particle size of the Pd NPs combined with the possible promoting effect of the CNTs could justify the observed higher activity of **Pd/CNTs** compared to **Pd/P-SiO_2**.

Next, the **PdCu/CNTs** and **PdCu/P-SiO_2** nanocatalysts were tested in the same catalytic reactions and the results are displayed in Table 2.

Table 2. Semi-hydrogenation of alkynes catalysed by bimetallic PdCu based catalysts: **PdCu/CNTs** (entries 1-4) and **PdCu/P-SiO_2** (entries 5-8).[a]

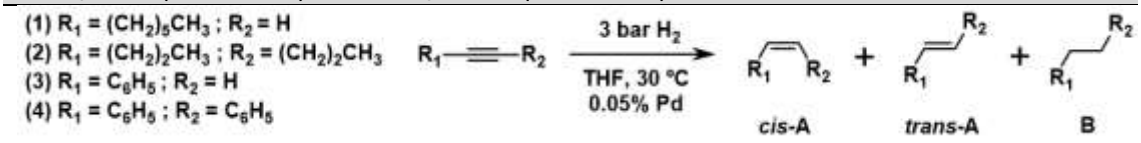

Entry	Substrate	t, h	Conv.%	Sel. Alkene %	Sel. B %	Sel. Isomers %	*Cis*:*Trans*
1	**1**	1.5	100	87	7	6	-
		3	100	74	13	13	-
2	**2**	0.5	100	100	0	0	92:8
		3	100	99	0	1	92:8
3	**3**	3	100	39	61	0	-
4	**4**	3	9	100	0	0	66:34
5	**1**	3	16	100	0	0	-
6	**2**	0.5	100	96	0	4	92:8
7	**3**	3	10	100	0	0	-
8	**4**	3	11	100	0	0	24:76

[a]Reaction conditions: 1.35 mmol of substrate, 0.05 mol% Pd, 5 mL THF, 600 rpm, 3 bar of H_2. Entries 1-4 for **PdCu/CNTs** and 5-8 for **PdCu/P-SiO_2**. Conversions and selectivities were determined by GC-MS spectrometry.

When **PdCu/CNTs** were used as catalysts in the semi-hydrogenation of 1-octyne (entry 1) full conversion was obtained at 1.5 h with 87% alkene selectivity. This latter value slightly decreased to 74% after 3 h of reaction. For 4-octyne (entry 2), full conversion was achieved at 0.5 h with 100% alkene selectivity and 91% *cis*-selectivity. Interestingly, after 3 h of reaction the alkene and *cis*-selectivity remained unchanged. The low evolution of the alkene selectivity and the *cis : trans* ratio after extended reaction times observed for 1 and 4-octyne is an indication of the superior performance of **PdCu/CNTs** in comparison to **Pd/CNTs**. Regarding the aromatic

substrates, full conversion at 3 h was obtained for phenylacetylene (entry 3) with 61% of the over-hydrogenation product. Curiously, for diphenylacetylene (entry 4) only a 9% of conversion was achieved after 3 h.

Similar to the trend observed for the series of Pd monometallic catalysts, lower activities were obtained for **PdCu/P-SiO$_2$** than its analogous **PdCu/CNTS**. Conversions as low as 16% for 1-octyne (entry 5), 10% for phenylacetylene (entry 7) and 11% for diphenylacetylene (entry 8) were obtained after 3h of reaction. On the contrary, for the case of 4-octyne (entry 6) full conversion was achieved at 0.5 h with 96% alkene and 92% *cis*-selectivities. The low activity evidenced by **PdCu/P-SiO$_2$**, could be attributed to the ultra-small size of the PdCu NPs and the moderating effect of Cu on the activity of the active Pd phase. Conversely, the higher activity exhibited by **PdCu/CNTs** could be mainly associated to the larger particle size of the PdCu NPs.

Finally, the copper-based materials were also tested in catalysis. However no activity was observed under the tested conditions (0.7 mol% Cu, 50 ºC and 3 h).

In conclusion, the introduction of Cu in the Pd structure to form a nanoalloy promotes the alkene selectivity by preventing over-hydrogenation and isomerisation processes. This observation is in agreement with a previous report where the alloying of Pd with Cu lower the hydrogenation activity and as such helps preventing overhydrogenation.[7a] It is important to highlight, that due to the structure sensitivity of the hydrogenation of alkynes, the particle size of the M-NPs may affect the activity of a catalyst, and that the particle size is also highly influenced by the nature of the support. In this study, it was observed that CNTs favoured the formation of larger NPs which resulted in more active catalysts when compared to those prepared on P-SiO$_2$ which generally contained ultra-small NPs.

When a recycling experiment was performed using the **PdCu/CNTs** catalyst, the semi-hydrogenation of 4-octyne could be performed in 6 consecutive runs without loss of activity nor selectivity to the alkene product, although a slight degree of cis/trans isomerisation was detected after the 4th run (Figure 7).

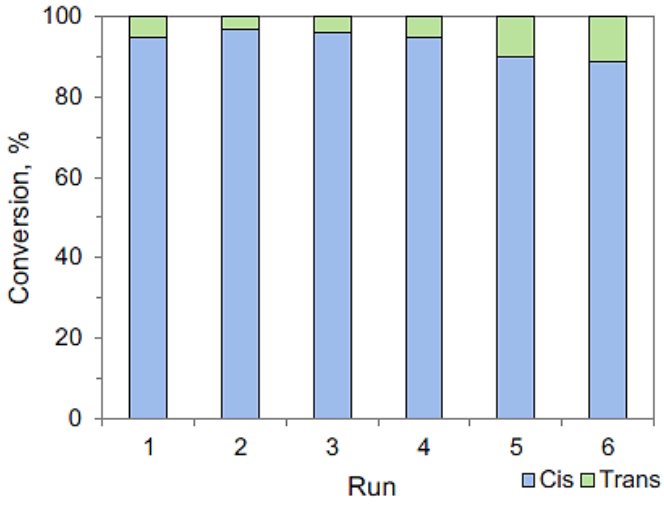

Figure *7*. Recycling of **PdCu/CNTs** catalyst in the semi-hydrogenation of 4-octyne.

4. Conclusions

A general methodology was employed for the preparation of two series of supported mono (Pd and Cu) and bimetallic (PdCu) nanoparticles on carbon nanotubes and phosphorus

functionalised silica. Variations in particle size of the M-NPs as a function of the support and the metallic composition indicated stronger metal-support interactions for the case of the CNTs supported series. For instance, the series of CNTs catalysts evidenced in general larger particle sizes than those supported on P-SiO_2 for equivalent metallic compositions.

These materials were tested in the selective hydrogenation of alkynes giving insights into the effect of the support and the active phase in the catalytic performance. The nanocatalysts supported on CNTs displayed a higher activity in comparison to those supported on P-SiO_2. This behaviour could be attributed to a combination of two effects: the larger particle size of the M-NPs supported on CNTs (considering that larger particles are generally more active in this reaction) and a possible electronic effect due to the graphitic nature of CNF.

In addition, the bimetallic catalyst **PdCu/CNTs** displayed a remarkable resistance against over-hydrogenation/isomerisation after full conversion of aliphatic alkynes, which is a consequence of the promoting effect of copper. These results evidence how the combination of several strategies (selection of the support, control of the particle size and the use of promoters) may result in highly structured materials with enhanced performance in catalysis.

This catalyst could moreover be recycled several times without loss of activity nor selectivity.

5. Acknowledgements

The authors acknowledge the Ministerio de Economia y Competividad and the Fondo Europeo de Desarrollo Regional FEDER (CTQ2016-75016-R, AEI/FEDER,UE, PID2019-104427RB-100), the Generalitat de Catalunya (SGR2014) and CNRS for financial support.

6. References

[1] a) G. Schmid, G. *Nanoparticles: From Theory to Applications* Weinheim, **2010**; b) M. Diaz de los Bernardos, S. Perez-Rodriguez, A. Gual, C. Claver, C.; C. Godard, C. *Chem. Commun.* **2017**, *53*, 7894-7897; c) J. A. Delgado, O. Benkirane, C. Claver, D. Curulla-Ferre, C. Godard, *Dalton Trans.* **2017**, *46*, 12381-12403.

[2] a) C. J. Jia, F. Schuth, *PCCP* **2011**, *13*, 2457-2487; b) M. E. Grass, Y. Zhang, D. R. Butcher, J. Y. Park, Y. Li, H. Bluhm, K. M. Bratlie, T. Zhang, G. A. Somorjai, *Angew. Chem. Int. Ed.* **2008**, *47*, 8893-8896.

[3] C. Hubert, E. G. Bile, A. Denicourt-Nowicki, A. Roucoux, *App. Catal. A Gen.* **2011**, *394*, 215-219.

[4] R. P. J. M. Basset, D. Roberto, R. Urgo, in *Modern surface organometallic chemistry*, Weinheim, **2009**.

[5] V. Vece, K. C. Szeto, M. O. Charlin, P. Rouge, A. De Mallmann, M. Taam, P.-Y. Dugas, M. Lansalot, F. D'Agosto, M. Taoufik, *Catal. Commun.* **2019**, *129*, 105715.

[6] a) J. Llop Castelbou, K. C. Szeto, W. Barakat, N. Merle, C. Godard, M. Taoufik, C. Claver, *Chem. Commun.* **2017**, *53*, 3261-3264; b) N. Popoff, J. Espinas, J. Pelletier, K. C. Szeto, J. Thivolle-Cazat, L. Delevoye, R. M. Gauvin, M. Taoufik, *ChemCatChem* **2013**, *5*, 1971-1977.

[7] a) D. A. Lomelí-Rosales, J. A. Delgado, M. Díaz de los Bernardos, S. Pérez-Rodríguez, A. Gual, C. Claver, C. Godard, *Chem. Eur. J.* **2019**, *25*, 8321-8331; b) L. Montiel, J. A. Delgado, M. Novell, F. J. Andrade, C. Claver, P. Blondeau, C. Godard, *ChemCatChem* **2016**, *8*, 3041-3044.

[8] a) D. Uzio, G. Berhault, *Cat. Rev.* **2010**, *52*, 106-131; b) S. Yang, C. Cao, L. Peng, J. Zhang, B. Han, W. Song, *Chem. Commun.* **2016**, *52*, 3627-3630; c) Y. K. Gulyaeva, V. V. Kaichev, V. I. Zaikovskii, A. P. Suknev, B. S. Bal'zhinimaev, *App. Catal. A Gen.* **2015**, *506*, 197-205.

[9] a) M. Crespo-Quesada, F. Cárdenas-Lizana, A.-L. Dessimoz, L. Kiwi-Minsker, *ACS Catal.* **2012**, *2*, 1773-1786; b) N. Semagina, M. Grasemann, N. Xanthopoulos, A. Renken, L. Kiwi-Minsker,

J. Catal. **2007**, *251*, 213-222.
[10] a) D. Mei, M. Neurock, C. M. Smith, *J. Catal.* **2009**, *268*, 181-195; b) M. García-Mota, J. Gómez-Díaz, G. Novell-Leruth, C. Vargas-Fuentes, L. Bellarosa, B. Bridier, J. Pérez-Ramírez, N. López, *Theor. Chem. Acc.* **2011**, *128*, 663-673; c) N. Lopez, C. Vargas-Fuentes, *Chem. Commun.* **2012**, *48*, 1379-1391; d) F. Studt, F. Abild-Pedersen, T. Bligaard, R. Z. Sørensen, C. H. Christensen, J. K. Nørskov, *Science* **2008**, *320*, 1320-1322; e) E. Vignola, S. N. Steinmann, B. D. Vandegehuchte, D. Curulla, P. Sautet, *J. Phys. Chem. C* **2016**, *120*, 26320-26327.
[11] a) A. Yarulin, I. Yuranov, F. Cárdenas-Lizana, D. T. L. Alexander, L. Kiwi-Minsker, *App. Catal. A Gen.* **2014**, *478*, 186-193; b) C. F. Calver, P. Dash, R. W. J. Scott, *ChemCatChem* **2011**, *3*, 695-697; c) T. Mitsudome, T. Urayama, K. Yamazaki, Y. Maehara, J. Yamasaki, K. Gohara, Z. Maeno, T. Mizugaki, K. Jitsukawa, K. Kaneda, *ACS Catal.* **2016**, *6*, 666-670.
[12] a) L. M. Bronstein, D. M. Chernyshov, I. O. Volkov, M. G. Ezernitskaya, P. M. Valetsky, V. G. Matveeva, E. M. Sulman, *J. Catal.* **2000**, *196*, 302-314; b) E. Sulman, V. Matveeva, A. Usanov, Y. Kosivtsov, G. Demidenko, L. Bronstein, D. Chernyshov, P. Valetsky, *J. Mol. Catal. A: Chem.* **1999**, *146*, 265-269; c) S. Wang, Z. Xin, X. Huang, W. Yu, S. Niu, L. Shao, *PCCP* **2017**, *19*, 6164-6168.
[13] M. Ren, C. Li, J. Chen, M. Wei, S. Shi, *Catal. Sci. Technol.* **2014**, *4*, 1920-1924.
[14] C. W. A. Chan, A. H. Mahadi, M. M.-J. Li, E. C. Corbos, C. Tang, G. Jones, W. C. H. Kuo, J. Cookson, C. M. Brown, P. T. Bishop, S. C. E. Tsang, *Nat. Commun.* **2014**, *5*, 5787.
[15] a) A. J. McCue, R. T. Baker, J. A. Anderson, *Faraday Discuss.* **2016**, *188*, 499-523; b) E. Buxaderas, M. A. Volpe, G. Radivoy, *Synthesis* **2019**, *51*, 1466-1472.
[16] a) A. Fedorov, H.-J. Liu, H.-K. Lo, C. Copéret, *J. Am. Chem. Soc.* **2016**, *138*, 16502-16507; b) N. Kaeffer, H.-J. Liu, H.-K. Lo, A. Fedorov, C. Copéret, *Chem. Sci.* **2018**, *9*, 5366-5371.
[17] A. Shaygan Nia, S. Rana, D. Döhler, F. Jirsa, A. Meister, L. Guadagno, E. Koslowski, M. Bron, W. H. Binder, *Chem. Eur. J* **2015**, *21*, 10763-10770.
[18] T. Ohba, H. Kubo, Y. Ohshima, Y. Makita, N. Nakamura, H. Uehara, S. Takakusagi, K. Asakura, *Bull. Chem. Soc. Jpn.* **2017**, *90*, 720-727.
[19] P. Tribolet, L. Kiwi-Minsker, *Catal. Today* **2005**, *105*, 337-343.
[20] a) Vanharde.R, F. Hartog, *Surf. Sci.* **1969**, *15*, 189; b) N. Semagina, A. Renken, L. Kiwi-Minsker, *J. Phys. Chem. C.* **2007**, *111*, 13933-13937; c) N. Semagina, A. Renken, D. Laub, L. Kiwi-Minsker, *J. Catal.* **2007**, *246*, 308-314; d) J. Hu, Z. Zhou, R. Zhang, L. Li, Z. Cheng, *J. Mol. Catal. A Chem.* **2014**, *381*, 61-69; e) D. Teschner, E. Vass, M. Havecker, S. Zafeiratos, P. Schnoerch, H. Sauer, A. Knop-Gericke, R. Schloegl, M. Chamam, A. Wootsch, A. S. Canning, J. J. Gamman, S. D. Jackson, J. McGregor, L. F. Gladden, *J. Catal.* **2006**, *242*, 26-37; f) M. Crespo-Quesada, A. Yarulin, M. Jin, Y. Xia, L. Kiwi-Minsker, *J. Am. Chem. Soc.* **2011**, *133*, 12787-12794; g) N. Semagina, L. Kiwi-Minsker, *Catal. Lett.* **2009**, *127*, 334-338.

Supporting Information

1. Reagents, materials and equipments

Metal precursor $Pd(dba)_2$, alkyne substrates and any other compounds were purchased from Sigma-Aldrich, Stream Chemicals or Across Organics and used without any further purification. Mesitylcopper (I) $(CuMes)_4$ was synthesised employing reported methodologies and stored in the glovebox.[1] Commercial CNTs (PR-24-XT-LHT, PYROGRAP®) were used as support. According to the manufacturer, these CNTs are synthesised from a Fe precursor as growth catalyst (Fe < 0.6 wt%). Nylon 6,6 membrane (Filter-Lab, 0.45 µm x 47 mm) were used to filter the nanoparticles. Tetrahydrofuran employed for synthesis and catalysis was taken form a solvent purification system (SPS) and refluxed under sodium/acetophenone till complete dryness (Karl-Fischer analysis evidenced <10 ppm of water after collection). Hexane was used directly as taken from the SPS. Any other solvent or reagent employed was reagent grade. Hydrogen (5.0) was purchased from Abello Linde. All the synthesis were performed under inert atmosphere inside the glovebox employing Fischer-Porter bottles. The work-ups were also performed inside the glovebox, as well as all the manipulations involving pure copper NPs catalysts.

Transmission electron microscopy (TEM) measurements were performed at the "Unitat de Microscopia dels Serveis Cientifico Tècnics de la Universitat Rovira i Virgili" in Tarragona with JEOL 1011 electron microscope operated at 100 kV with resolution of 3 Å. The particles size distributions were determined by a manual analysis of enlarged images. At least 200 particles on a given grid were measured in order to obtain a statistical size distribution and a mean diameter.

Scanning Transmission Electron Microscopy - High Angle Annular Dark Field (STEM-HAADF) images were obtained in a probe-corrected Titan (FEI) at a working voltage of 300 kV, coupled with a HAADF detector (Fischione). In this mode, the intensity of the signal is proportional to the square of the atomic number (Z^2), therefore heavier elements appear with a much brighter contrast than lighter elements, like carbon or silicon. In addition, with the aim to analyse the chemical composition of the materials, X-ray Energy Dispersive Spectra (EDS) were obtained with an EDAX detector. The samples were dispersed in THF and a small amount of solution was then deposited on a Cu-C grid. The STEM equipment is located at the "Advanced Microscopy Laboratory of the Instituto de Nanociencia de Aragón" in Zaragoza.

X-ray Diffraction (XRD) measurements were made using a Siemens D500 diffractometer (Bragg-Brentano parafocusing geometry and vertical θ-θ goniometer) fitted with a curved graphite diffracted-beam monochromator, incident and diffracted-beam Soller slits, a 0.06º receiving slit and scintillation counter as a detector. The angular 2θ diffraction range was between 25 and 90º. The data were collected with an angular step of 0.05º at 16 s per step and sample rotation. A low background Si (510) wafer was used as sample holder. Cukα radiation was obtained from a copper X-ray tube operated at 40 kV and 30 mA. Gas chromatography analysis was carried out on an Agilent 7890A with a MS 5975C detector using a Colum HP-MS (30 m, 0.25 mm, 0.25 µm).

Inductively coupled plasma-atomic emission spectroscopy (ICP-AES) analysis were performed on an Ethos Easy Advanced microwave digestion system. As a general procedure, 5 mg of sample were charged in Teflon liners followed by 10 mL of a concentrated acid mixture of HNO_3 and HF (4:1). The heating program started with the

increase from room temperature to 200 ºC during 30 min (approx. 6ºC/min) and followed with an isotherm at 200 ºC during 1 h more. The irradiation power during all the run was automatically controlled by the equipment to fit the temperature program. After a typical digestion, the reactors were open, and the homogeneity of the solution was examined. The solutions were transferred to volumetric flasks of 50 mL and the liners washed exhaustively with milli-Q water. Finally, the obtained solutions were analysed by ICP-AES. Quantification of Pd, Cu and P is performed by comparison with the respective calibration curve constructed in the range of 0-20 ppm.

Gas chromatography mass spectrometry (GC-MS) was carried out on a HP 6890A spectrometer, with HP-5 column (0.25 nm x 30 m x 0.25 μm).

2. Synthesis of metal nanoparticles

The series of the supported catalysts were synthesized by chemical reduction/decomposition of the metal precursor(s) under hydrogen based on a reported method developed in our group. In the following paragraphs the detailed synthesis of each NPs is described.

2.1. Preparation of mono and bimetallic Pd, Cu and PdCu nanoparticles supported on phosphorus functionalised silica

Pd/P-SiO_2. Under nitrogen atmosphere, in a 250 mL Fischer-Porter 150 mg of phosphorus functionalised silica (P-SiO_2), 40.5 mg of $Pd(dba)_2$ (5 wt%, 0.07 mmol) and 7.4 mg of PPh_3 (0.028 mmol) were added followed by 30 mL of dry THF. The Fischer-Porter bottle was then tightly closed and pressurised with 3 bars of H_2 and left at room temperature at 700 rpm. The initial red and solution turned black in one hour. The mixture was stirred during 16 h, then the reactor was depressurised at air atmosphere and the dispersion was introduced in a centrifuge. The floating THF was removed and dry *n*-hexane added for washing, then the tube was shook and centrifuged again. The washing process with *n*-hexane was repeated 3 times in total and the resulting material dried in the air atmosphere. A sample of solid was finally suspended in dry *n*-hexane in order to prepare the grid for TEM analysis.

TEM: mean size [0.91 ± 0.31] nm.

XRD: Pd-fcc crystalline nanoparticles

ICP: 4.4 wt% Pd, 1.0 wt% P

PdCu/P-SiO_2. Under nitrogen atmosphere, in a 250 mL Fischer-Porter reactor 150 mg of P-SiO_2, 40.5 mg of $Pd(dba)_2$ (5 wt%, 0.07 mmol), 21.8 mg of MesCu (5 wt%, 0.119 mmol) and 19.8 mg of PPh_3 (0.075 mmol) were added followed by 30 mL of dry THF. The Fischer-Porter bottle was then tightly closed and pressurised with 3 bars of H_2 and put in a preheated oil bath at 70 ºC and 700 rpm. The initial red solution turned black in three hours. The mixture was stirred during 16 h, then the reactor was depressurised and entered into a glovebox, the reaction mixture was transferred into a flask in order to concentrate the solution under reduced pressure. A sample from the black powder obtained was diluted in dry *n*-hexane to prepare the carbon- covered grid for TEM analysis.

TEM: mean size [1.48 ± 0.39] nm.

XRD: Pd/Cu nanoalloy.

ICP: 3.3 wt% Pd, 3.8 wt% Cu, 1.7 wt% P.

Cu/P-SiO_2. Under nitrogen atmosphere, in a 250 mL Fischer-Porter reactor 21.5 mg of MesCu (5 wt%, 0.119 mmol) and 12.4 mg of PPh_3 (0.047 mmol) were added followed by 30 mL of dry THF. The Fischer-Porter bottle was then tightly closed and pressurised with 3 bars of H_2 and put in a preheated oil bath at 70 ºC and 700 rpm. The initial white solution turned black in three hours. The mixture was stirred during 16 h, then the reactor was depressurised and entered into a glovebox, the reaction mixture was transferred into a flask in order to concentrate the solution under reduced pressure. A sample from the black powder obtained was diluted in dry *n*-hexane to prepare the carbon-covered grid for TEM analysis.

TEM: mean size [2.14 ± 0.73] nm.

XRD: Cu-fcc crystalline nanoparticles

ICP: 4.8 wt% Cu, 1.7 wt% P.

2.2. Preparation of mono and bimetallic Pd, PdCu and Cu nanoparticles supported on carbon nanotubes Pd/CNTs. Under nitrogen atmosphere, in a 500 mL Fischer-Porter bottle 150 mg of CNTs, 40.5 mg of $Pd(dba)_2$ (5 wt%, 0.07 mmol) and 7.4 mg PPh_3 (0.028 mmol) were added followed by 30 mL of dry THF. The Fischer-Porter bottle was then tightly closed and pressurised with 3 bars of H_2 and put in a stirrer with at room temperature at 700 rpm. The initial red solution turned black in one hour. The mixture was stirred during 16 h, then the reactor was depressurised at air atmosphere and 30 mL of dry *n*-hexane was added to the reaction mixture and stirred for 20 min more. After the *n*-hexane addition, a small amount (5 drops approx.) of the resulting dispersion was deposited on a carbon-covered copper grid for TEM analysis. The rest of the solution was then filtered through a Nylon 6,6 membrane and washed with dry *n*-hexane in order to obtain the resulting material which was dried under air atmosphere to remove the residual solvent.

TEM: mean size [2.57 ± 0.58] nm.

XRD: Pd-fcc crystalline nanoparticles

ICP: 4.4 wt% Pd, 0.3 wt% P.

PdCu/CNTs. Under nitrogen atmosphere, in a 250 mL Fischer-Porter bottle 150 mg of CNTs, 40.53 mg of $Pd(dba)_2$ (5 wt%, 0.07 mmol), 21.75 mg of MesCu (0.119 mmol) and 19.7 mg of PPh_3 (0.075 mmol) were added followed by 30 mL of dry THF. The Fischer-Porter bottle was then tightly closed and pressurised with 3 bars of H_2 and put in a preheated oil bath at 70 ºC and 700 rpm. The initial red solution turned black in three hours. The mixture was stirred during 16 h, then the reactor was depressurised and entered into a glovebox, 30 mL of *n*-hexane was added to the reaction mixture and stirred for 20 min more. After the *n*-hexane addition, a small amount (5 drops approx.) of the resulting dispersion was deposited on a carbon-covered copper grid for TEM analysis. The rest of the solution was then filtered through a Nylon 6,6 membrane and washed with dry *n*-hexane in order to obtain the PdCu-NPs/CNTs, the final product was dried in an open vial inside the glovebox to remove the residual solvent.

TEM: mean size [2.56 ± 0.62] nm.

XRD: Pd/Cu nanoalloy.

ICP: 3.3 wt% Pd, 5.7 wt% Cu, 0.5 wt% P.

Cu-/CNTs. Under nitrogen atmosphere, in a 250 mL Fischer-Porter bottle 150 mg of CNTs, 21.5 mg of MesCu (5 wt%, 0.119 mmol) and 12.4 mg PPh_3 (0.047 mmol) followed were added by 30 mL of dry THF. The Fischer-Porter was then tightly closed and pressurised with 3 bars of H_2 and put in a preheated oil bath at 70 ºC and 700 rpm. The initial white solution turned black in three hours. The mixture was stirred during 16 h, then the reactor was depressurised and entered into a glovebox, 30 mL of *n*-hexane was added to the reaction mixture and stirred for 20 min mores. After the n-hexane addition, a small amount (5 drops approx.) of the resulting dispersion was deposited on a carbon-covered copper grid for TEM analysis. The rest of the solution was then filtered through a Nylon 6,6 membrane and washed with dry *n*-hexane in order to obtain the Cu-NPs/CNTs as a black powder, the final product was dried in an open vial inside the glovebox to remove the residual solvent.

TEM: mean size [2.41 ± 0.63] nm.

XRD: Cu-fcc crystalline nanoparticles

ICP: 6 wt% Cu, 0.4 wt% P.

3. General procedure for the semi-hydrogenation of alkynes

The hydrogenation reactions were carried out in a five-position Parr reactor provided with glass liners. In a typical experiment, the glass tube was charged with the corresponding amount of a previously prepared suspension of the nanocatalyst and the substrate in 5 mL of THF. Hydrogen gas was then introduced at the desired pressure. The reaction was then stirred at 600 rpm at the defined temperature (heated using a water bath). The reactor was depressurised temporarily at defined reaction times (50 µL of sample which was diluted in 5000 µL of absolute ethanol and analysed by GC-MS spectrometry). After the sampling, the reactor was closed and pressurised to continue the reaction.

Recycling experiments

In the first run, the catalytic reaction was performed as above mentioned. Between each run, the PdCu/CNTs nanoparticles were isolated by centrifugation. The supernatant was removed and analysed by GC- MS while the PdCu/CNTs nanoparticles were washed three times with 10 ml of cold and deoxygenated hexane, brought to dryness under reduced pressure, and later redispersed in THF. The substrate was then added for the next catalytic cycle.

4. Characterisation

4.1. Supported M-NPs on functionalised silica

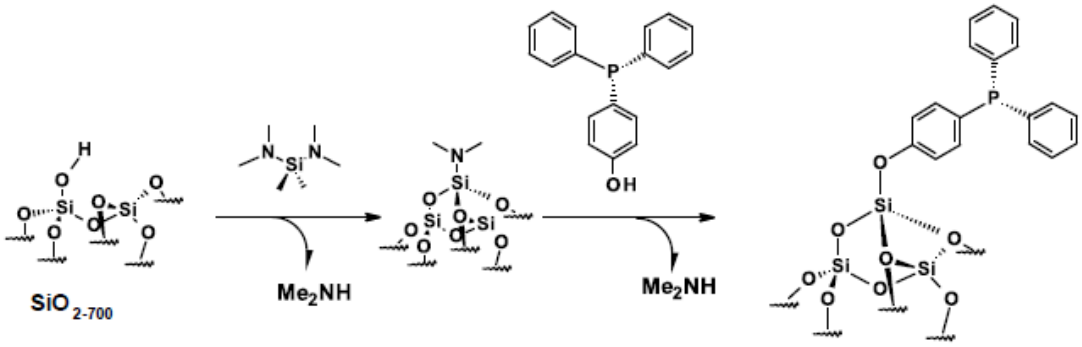

Figure 1. Synthesis of the phoshporus functionalised silica employed as support.[2]

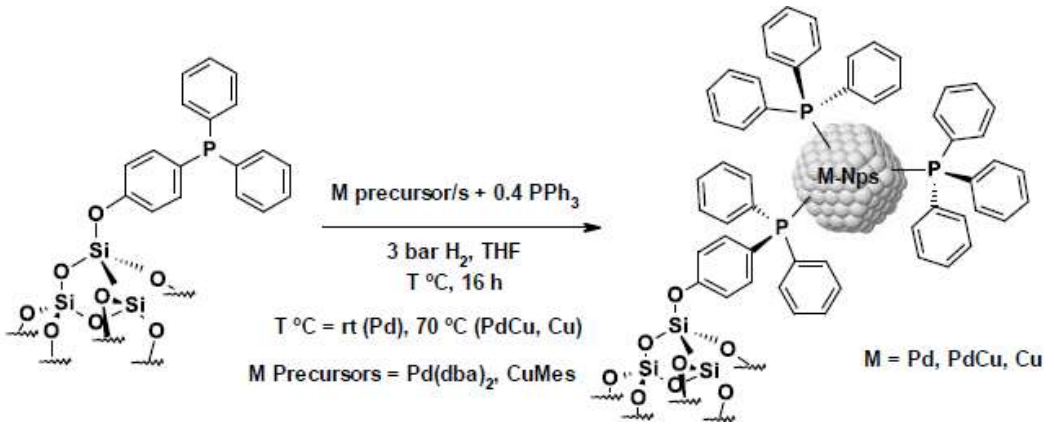

Figure 2. Synthesis of the supported monometallic and bimetallic M-NPs (M = Pd, PdCu and Cu) on functionalised silica.[2]

4.1.1. XRD

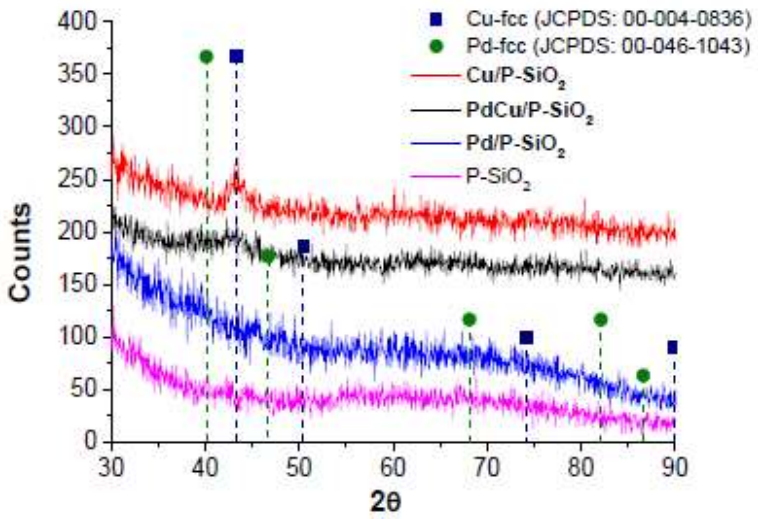

Figure 3. XRD patterns for the metal nanoparticles series: M-NPs/P-SiO_2 (M = Pd, PdCu, Cu) and for the phosphorus functionalised silica support (P-SiO_2)

Table 1. Crystallographic data for reference Pd and Cu fcc metallic phases

	d spacing, Å	
Plane (hkl)	Pd (JCPDS: 00-046-1043)	Cu (JCPDS: 00-004-0836)
111	2.246	2.087
200	1.945	1.808
220	1.375	1.278

Table 2: Crystallographic experimental data of metallic NPs from Pd/P-SiO2, PdCu/SiO2 and PdCu/CNTs extracted from FFT analysis of STEM images.

	d spacing, Å		
Plane (hkl)	**Pd/P-SiO2**	**PdCu/P-SiO2**	**PdCu/CNTs**
111	2.468	2.406	2.251
200	2.192	2.067	1.826
220	1.454	1.431	

4.1.3. ICP

Table 3. ICP results for the supported M-NPs (M = Pd, PdCu, Cu) on phosphorus functionalised slica.

Catalyst	Nominal metal loading wt%	ICP metal loading wt%
$Pd/P\text{-}SiO_2$	5	4.4
$PdCu/P\text{-}SiO_2$	5-Pd	3.3-Pd
	5-Cu	3.8-Cu
$Cu/P\text{-}SiO_2$	5	4.8

4.2. Synthesis of supported M-NPs on carbon nanotubes

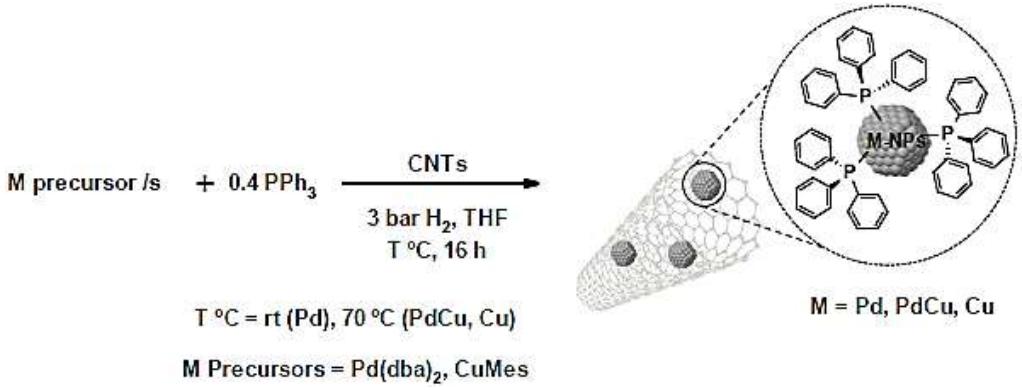

Figure 4. Synthesis of the carbon nanotubes supported monometallic and bimetallic M-NPs/CNTs (M = Pd, PdCu, Cu) catalysts

4.2.1. XRD

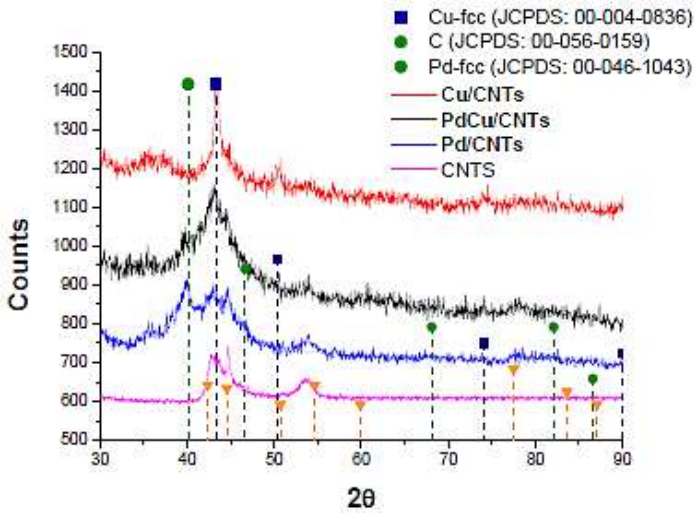

Figure 5. XRD patterns for the metal nanoparticles series: M-NPs/CNTs (M = Pd, PdCu, Cu) and for the carbon nanotubes material support.

4.2.3. ICP

Table 4. ICP results for the supported M-NPs (M = Pd, PdCu, Cu) on carbon nanotubes

Catalyst	Nominal metal loading wt%	ICP metal loading wt%
Pd/CNTs	5	4.4
PdCu/CNTs	5-Pd	3.3-Pd
	5-Cu	5.7-Cu
Cu/CNTs	5	6

4.3. Comparison between the CNTs ans P-SiO_2 supported catalysts series

Table 5. Mean diameter and ICP results for the supported catalysts.

M-NPs	Metal Precursor	Support	Metal wt% loading on M-NPs/support	Metal %wt loading by ICP of M-NPs/support	Mean diameter / nm
Pd	$Pd(dba)_2$	P-SiO_2	5	4.4	0.92 ± 0.31
Pd	$Pd(dba)_2$	CNTs	5	4.4	2.57 ± 0.58
PdCu	$Pd(dba)_2$/CuMes	P-SiO_2	5-Pd	3.3	1.49 ± 0.39
			5-Cu	3.8	
PdCu	$Pd(dba)_2$/CuMes	CNTs	5-Pd	3.3	2.56 ± 0.62
			5-Cu	5.7	
Cu	CuMes	P-SiO_2	5	4.8	2.14 ± 0.74
Cu	CuMes	CNTs	5	6	2.41 ± 0.63

[1] Eriksson, H.; Håkansson, M. *Organometallics* **1997**, *16*, 4243.

[2] Didelot, C., Master's Thesis, *Chimie organométallique de surface: préparation de nanoparticules supportées, application à la catalyse*, Université Claude Bernard, Lyon, **2017**. A paper on this work is in preparation.

Graphical Abstract

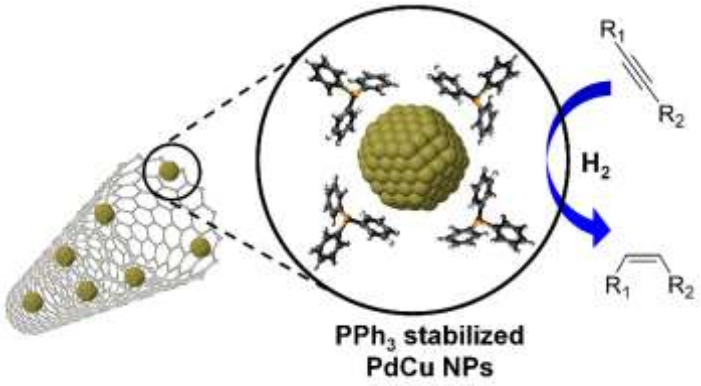

Table of contents

A one pot methodologie for the preparation for triphenylphosphine stabilized Pd, Cu and PdCu nanocatalyst supported on carabon nanotubes and phosphosurs functionalised silica is presented here. The catalysts were tested in the semi-hydrogenation of alkynes. Differences in reactivity were correlated with the particle size and composition of the nanoparticles and the nature of the support.